

**Gas Adsorption Studies of MCM-41 Porous  
Material: One-Dimensional Helium Confinement  
in a Mesoporous Silica**

**Jaiden Medina**  
**Indiana University Bloomington**  
**July 2023**

**Abstract:**

The understanding of the 1-dimensional properties of substances has grown in the past few years. More specifically it looks at the quantum state of matter known as a 'superfluid'. To access this state, weight must be condensed to such a small volume that the material no longer interacts with each other or other objects in three dimensions, it acts in only one dimension. A substance used most often to grow the understanding of superfluids is the isotope helium-4, due to its inability to become a solid, no matter the temperature or pressure it is under, going from a liquid state of matter to a quantum liquid. To observe these properties and to better understand them a series of computational coding and experimental processes, such as x-ray diffraction and gas isotherm was used on MCM-41 material created in the lab. The structure was found, the pore diameter calculated, and the helium-4 isotope was pumped into the mesoporous material. Then the one-dimensional properties of helium-4 were observed and recorded. The observations could lead to a host of benefits in the pharmaceutical, medical, biosensor, thermal energy storage, water/gas filtration, imaging fields, and astrophysics world. It could lead to the creation of the

*Theory of Everything.*

**Introduction:**

In the previous few decades, there has been an uptick in the research that has been devoted to progressing nanotechnology and nanoscience since its inception in 1952. This is especially prevalent in the progress of synthesis, characterization, evaluation of properties, and a wide range of applications in catalysis, adsorption, separation, control of environmental pollution, controlled release of drugs, and sensors aiming at the improvement of quality of daily life of society (Costa, 2019). There has been a particular focus on mesoporous silicas that have gained the interest of scientists due to their promising and vast range of uses in the pharmaceutical, medical, biosensors, thermal energy storage, water/gas filtration, and imaging fields (Costa, 2019). The most widely used and well-known of the mesoporous silicates is MCM-41.

MCM-41 (Mobil Composition of Matter No.41) was first reported to be synthesized by scientists working for the Mobil Oil Corporation in 1992. The development of MCM-41 coincided with the development of a family of mesoporous silicates developed during this time, aptly named M41S. According to the book “Mesoporous and Microporous Materials Vol.291”, this family of silicates is all synthesized under primary conditions in the presence of alkylammonium surfactants and a silica source whose pore size comprises the range of 3–10 nm. Furthermore, the properties of MCM-41 that make it unique are its hierarchical structure consisting of cylindrical pores in a hexagonal lattice, with space-group symmetry ( $P6mm$ ) and a unidirectional system of pores which has a diameter between  $3.0 \pm 0.3$  nanometers. (Warren, 2019) as shown in **Figure one**. Other widely known members of the M41S family include MCM-48, which has a cubic structure, with space-group symmetry, and pores that are

interconnected in a 3D system, and MCM-50, which contains a lamellar structure, without space-group symmetry, consisting of silica layers in the presence of double layers of surfactant.

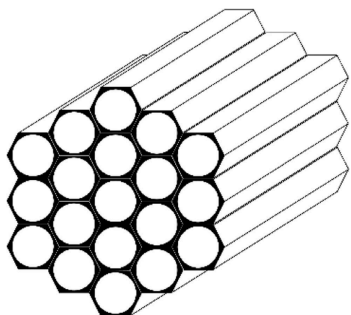


**Figure one:** Pore structure of MCM-41

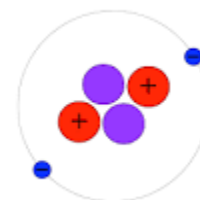


**Figure two:** The physical structure of isotope 4 of helium-4; includes two protons, two neutrons, and two electrons

When studying gas adsorption in mesoporous silicates any gas can be used, but the isotope helium-4 is one of the most studied because of the isotope's unique properties. Helium-4 derives its special properties from its atomic structure. As shown in **Figure two**, Helium-4 is composed of two neutrons, two protons, and two electrons. Due to this fact, this means that Helium-4 is a type of particle called a boson particle, which is known to occupy the same energy levels as its neighboring particles. This becomes especially important when scientists strive to reach a phenomenon called “superfluidity”. It means when a substance’s atoms or particles come into a superfluid state, all atoms or particles within the substance occupy the same energy level. Moreover, this quantum state changes the phase behavior of the substance. In this state, the superfluid has infinite thermal conductivity, superconductivity, and zero viscosity. Furthermore, this means that all of the particles and atoms act in unison with one another, instead of having a

sense of randomness. The superfluidity properties of Helium-4 were explained schematically by Fritz London and then in detail by Lev Landau in 1962. Commonly, to access the superfluidity processes of Helium-4 one would have to cool down the isotope to 2.1 kelvin, or -271.05 degrees Celsius, colder than the deepest regions of space. This is significant because this temperature is very close to the coldest temperature mankind can reach, zero kelvin, otherwise known as absolute zero. To achieve this temperature scientists require special machinery. To avoid this obstacle scientists turn to the ideal gas law. The ideal gas law is shown below:

$$PV = nRT$$

The ideal gas law shows that by increasing pressure (P) and reducing the volume (V) of the pores in the MCM-41 one can access the superfluid properties of gas and for this instance Helium-4. The Ideal gas law was formulated in 1663 by Robert Boyle to explain the simple mathematical relationship between pressure and volume. He implies that as pressure increases, volume decreases by the same proportion implying the product, PV, is constant. This becomes especially important when increasing pressure and decreasing volume have the same effect as essentially freezing Helium-4 under confinement (within the pore). It is also important to note that Helium and all of its isotopes are unable to freeze into a solid state, further emphasizing the uniqueness of Helium. Restricting helium-4 to such a small volume reduces its capability to interact with other objects. In such a small volume the helium-4 does not act in three dimensions or even two dimensions it acts in the one-dimensional plane. What this means is that unlike in a three-dimensional spectrum where the particles of an atom are freely able to move past one another and jump into separate energy states, in a one-dimensional spectrum all of the particles occupy the same low-energy state and can not move past each other; they all act in unison. This

is why the isotope helium-4 being a boson particle is important. This also changes the way it interacts with objects as well. For example, in this state helium-4 would be able to pour itself out of a container while the container is upright or be able to leak through the most microscopic of cracks in a container.

Putting everything together, understanding the properties of Helium-4 along with the definition of superfluidity and the ideal gas law, one-dimensional containment, and the properties of MCM-41 can lead to the desired results, discovery, and discussion within this field of science and physics can lead to tremendous leaps in the future of mankind. The discoveries from this particular field of study are hypothesized to be the catalyst to the creation of batteries that never degrade, better superconductors, and vastly improved supercomputers, many times greater than the ones in use today. But the discoveries don't only help mankind on Earth but better help humanity understand the universe. The cores of Neutron Stars are thought to be made up of superfluids and the universe is hypothesized to be a superfluid. If these prove to be true this can lead to the completion of a "Theory of Everything". The Theory of Everything is a term for the ultimate theory of the universe—a set of equations capable of describing all phenomena that have been observed, or that will ever be observed on a microscopic and macroscopic level. (Costa, 2019).

## **Gas Adsorption Studies of MCM-41 Porous Material Literature Review**

The study of physics and more specifically the field of theoretical physics and nanophysics has grown and evolved over the years. Physicists have sought to understand the quantum properties of materials either through the reduction of temperature or the confinement of the material while increasing pressure. The focus of this study is one-dimensional helium confinement in a mesoporous silica structure. There have been many studies on the research of gas adsorption, x-ray diffraction, or the synthesis of the materials in the M41S. Still, there are not many studies have researched all of these components together. Combining these aspects can lead to many great advancements in our everyday life in the medical, pharmaceutical, defense, and scientific world. But there are benefits on a universal scale and they can lead to great advancements in the future of mankind in space exploration.

The purpose of this literature review is to emphasize the research that takes place in gas adsorption studies of MCM-41 porous material. This review will be broken down into three sections. In the first section of this review, the synthesis of MCM-41 will be discussed, and the disparities in detail between sources. In the second section of this review, the actual understanding of the one-dimensional spectrum and the confinement of substances within MCM-41. In the final section, gas adsorption and X-ray scattering will be discussed.

In the early 1990s scientists at Mobil Oil Corporation, it has synthesized the first ordered mesoporous silicate materials which are known as the M41S family (Costa, 2020). MCM-41 was created in 1992 by scientists working for the Mobil Oil Company, known nowadays as Mobil. MCM-41 is the most well-known of these materials and contains a hexagonal structure, with space-group symmetry ( $P6mm$ ) and a unidirectional system of pores (Costa, 2020). Being the most popular member of the M41S family means that there have been many different synthesis

methods. Each one of the synthesis methods does contain many of the same ingredients such as CTAB, the surfactant, TEOS, the most commonly used silica source, ethyl alcohol, and deionized water. The synthesis used for this research derived from “Int. Nano Letter, Vol 1, January 2011, pp 34-37 by Mohammad Teymouri, Abdolrauf Samadi-Maybodi, Amir Vahid”. This synthesis method was specifically chosen because this synthesis method included the molar concentration along with the molarity of each substance that was used during the experiment. To note, the paper, *MCM-41, MCM-48, and related mesoporous adsorbents: their synthesis and characterization* by D. Kumar, K. Schumacher, C. du Fresne von Hohenesche\*, M. Grün, and K.K. Unger did also include the molarity and molar concentration of the substances involved in synthesis but the experimental results differed. The difference in results of these papers that both claim to have the correct synthesis method of MCM-41 is the peer review process. Although the article is peer-reviewed, it may not have been reviewed by chemists but by physicists who didn’t understand the substantial consequence of the differing concentrations of the substances involved. This difference will be explained further in the discussion section. Another problem with deriving a method of synthesis is that some papers lacked the necessary detail involved. This could be due to the focus of the article not being synthesized or this section being overlooked in the peer-review process.

According to an article titled an article titled *Experimental Realization of One Dimensional Helium*, “The realization of experimental platforms exhibiting one-dimensional (1D) quantum phenomena has been elusive due to their inherent lack of stability, with a few notable exceptions including spin chains, carbon nanotubes, and ultracold low-density gases.”. This has puzzled scientists for ages, ever since Pyotr Leonidovich Kopitsa, the person credited with the discovery of the quantum state of superfluidity. Models have been made in the 2D and

3D spectrum, but not the first dimension. This is because “The resulting excitations of confined  $^4\text{He}$  are qualitatively different than 3D and 2D superfluid helium...” (Del Maestro 2018). There are two isotopes of helium chosen to conduct research into one-dimensional superfluid confinement. “The helium isotopes  $^3\text{He}$  and  $^4\text{He}$  have long served as model systems for precision test of theories of strongly interacting quantum matter and phase transitions for bosons, fermions, and mixed statistics systems.” (Del Maestro 2018). Helium can achieve this due to its particle orientation when it reaches this quantum state, it becomes a boson particle. This means that it occupies the same energy level as all of the particles surrounding it. When confined in such a tight volume, such as within MCM-41 micelles, superfluidity can be truly reached and observed. Special properties in this state include zero viscosity, zero interactions between itself and its container, and infinite inertia. Understanding these properties can lead to a host of benefits.

To characterize, or verify if the helium containment object is MCM-41, there are two main ways this is accomplished. Through powder X-ray diffraction and gas adsorption isotherm. Powder X-ray diffraction is when photons are shot at a sample and then bounce off of the sample back onto a detector. When a photon interacts with the material and not open space it is scattered into X-rays which are read by the detector. For MCM-41 three peaks are expected if synthesized correctly and this can tell us if there is a hexagonal structure involved. The other way to characterize MCM-41 is through a gas adsorption isotherm. The gas adsorption isotherm puts gas on top of an MCM-41 sample and detects whether the gas attaches to the surface of the porous material. This can be increased or decreased depending on the temperature and the pressure that is in the gas adsorption isotherm. The average pore size and the average pore diameter can be calculated from these results.

### Bibliography

Del Maestro, A., Nichols, N. S., Prisk, T. R., Warren, G., & Sokol, P. E. (2017). *Experimental Realization of One Dimensional Helium*, 1–6.

Department of Physics and Astronomy, University of Tennessee, Knoxville, TN 37996, USA; Min H. Kao Department of Electrical Engineering and Computer Science, University of Tennessee Knoxville, TN 37996, USA Data Science and Learning Division, Argonne National Laboratory, Argonne, Illinois 60439, USA Department of Physics, University of Vermont, Burlington, VT 05405, USA Materials Science Program, University of Vermont, Burlington, VT 05404, USA Center for Neutron Research, National Institute of Standards and Technology, Gaithersburg, MD 20899-6100, USA Department of Physics, Indiana University, Bloomington, IN 47408, USA

Gabelman, A. (2017). Adsorption Basics. *Adsorption Basics: Part 1*, 48–53.

Gabelman Process Solutions, LLC

Kumar, D., Schumacher, K., du Fresne von Hohensche, C., Grün, M., & Unger, K. K. (2001). Colloids and Surfaces A: Physicochemical and Engineering Aspects. *MCM-41, MCM-48 and Related Mesoporous Adsorbents: Their Synthesis and Characterisation*, 187–188, 109–116.

Institut für Anorganische Chemie und Analytische Chemie, Johannes Gutenberg-Universität, Duesbergweg 10-14, 55128 Mainz, Germany

Solovyov, L. A., Belousov, O. V., Dinnebier, R. E., Shmakov, A. N., & Kirik, S. D. (2003). *J. Phys. Chem B* 2005. *X-Ray Diffraction Structure Analysis of MCM-48 Mesoporous Silica*, 109, 3233–3237.

Institute of Chemistry and Chemical Technology, 660049 Krasnoyarsk, Russia, Max-Planck Institute for Solid State Research, Heisenbergstrasse 1, D-70569 Stuttgart, Germany, and Borekov Institute of Catalysis, 630090 Novosibirsk, Russia

Tan, Y., & O'Haver, J. H. (2004). *Journal of Colloid and Interface Science*. *Use of the BET Adsorption Isotherm Equation to Examine Styrene Adsorption by Nonionic Surfactants at the Water-Silica Interface*, 279, 289–295.

Department of Chemical Engineering, the University of Mississippi, University, MS 38677, USA

Teymouri, M., Samadi-Maybodi, A., & Vahid, A. (2011). *Int. Nano Letter*. *A Rapid Method for the Synthesis of Highly Ordered MCM-41*, 1, 34–37.

**Methodology:****1. Experimental****1.1. Materials**

MCM-41 synthesis was carried out using deionized water as a base for the solution, *n*-cetyltrimethylammonium bromide (CTAB) as a template and surfactant, tetraethoxysilane (TEOS) as a silicon source, ammonium hydroxide as a pH corrector (ACS grade 28-30%, VWR chemicals), ethyl alcohol to help as a surfactant (bond to hydrophilic side)(200 proof, Phramco), and sodium acetate trihydrate as a pH corrector. Other materials that were used during the experimental process were 2 150 mL glass beakers, one to measure the weight of all of the chemicals and materials used and another beaker to measure the materials before they are transferred to the other beaker. Other materials involved were 2 plastic boats, one to transfer the CTAB and another to transfer the sodium acetate trihydrate, a magnetic stirrer, parafilm, a metallic scoop/scrapper, a scale (Adventurer SL), a stir plate (VWR hotplate/stirrer), and paper towels to keep a clean workplace. After the initial synthesis, a Teflon container + larger stainless steel container to house the Teflon container was used in the autoclave and a quartz tube was used in the tube furnace for calcination.

**1.2. Synthesis****1.2.1. Rapid Synthesis of highly ordered MCM-41 porous material**

This rapid method for the synthesis of highly ordered MCM-41 was derived from a journal article titled, *Int. Nano Letter, Vol 1*, written by Mohammad Teymouri, Abdolrauf

Samadi-Maybodi, and Amir Vahid in 2011. The highly ordered MCM-41 was synthesized by dissolving 0.461 grams of ethyl alcohol, also known as ethanol, in 27.931 grams of deionized water. Deionized water is water that is purified by removing all of the ions present in the water, most of which are salts. The ethyl alcohol was added to the solution to bind to the surfactant used in this synthesis and help loosely hold the structure of the MCM-41 until calcination. After the ethyl alcohol was dissolved entirely, 0.802 grams of *n*-cetyltrimethylammonium bromide, which will be referred to as CTAB, was added to the solution. Pay special attention that none of the CTAB sticks to the walls of the beaker and all particles fall into the solution. The CTAB will act as the surfactant which will loosely hold the structure of the MCM-41 until it is calcined. After the CTAB was added, 0.028 grams of sodium acetate trihydrate was added to the solution. Similar to the CTAB, pay special attention that all contents fall into the solution. The sodium acetate trihydrate is acidic and will correct the pH of the solution so the micelles of the MCM-41 will locate themselves in the correct hexagonal structure. After the sodium acetate trihydrate was added to the solution, 3.854 grams of ammonium hydroxide (NH<sub>4</sub>OH) was also added. Quickly add the ammonium hydroxide before it evaporates. Ammonium hydroxide is also used as a pH corrector. Once all of the ingredients were added, the solution was stirred vigorously until the solution was homogeneous and clear. Following this process, 2.083 grams of tetraethyl orthosilicate, referred to as TEOS, was added to the newly mixed solution. The TEOS is the silica source in this synthesis. The TEOS will use the micelles as a scaffolding to form the correct structure. The molar composition of the solution was 1 M TEOS; 0.22 M CTAB; 0.034 M sodium acetate trihydrate; 11 M ammonium hydroxide; 1 M ethyl alcohol; 155 M deionized water. The solution was covered with a piece of clear parafilm to prevent evaporation and was left to stir for 24 hours. After this, the solution was filtered to remove excess moisture from the

gel. The gel was left to filter overnight to get the substance as dry as possible before placing it in the autoclave. The next day, the material was put into a Teflon container which was then placed in a stainless steel container which was then placed in the autoclave at 125 degrees Celsius for 24 hours. After 24 hours, the material was calcined at 500 degrees Celsius for 8 hours in a tube furnace to remove the surfactant. The tube furnace was heated up to 0.82 degrees Celsius per minute until it reached the desired temperature, at which point it continued for another 8 hours.

### 1.3. Characterization

The sample was characterized to verify that the synthesized material was indeed MCM-41. To observe the structure of the material the material was placed into an x-ray scattering machine that contained a copper anode. Copper K- $\alpha$  is an X-ray energy frequently used on lab-scale X-ray instruments. The energy is 8.04 keV, which corresponds to an x-ray wavelength of 1.5406 Å. The x-ray diffractometer measured data from an angle of 1.5 degrees to 7 degrees while the sample was on a spinning plate going at 4 rotations per second. This specific angle measurement was chosen due to the fact that since the structure of the material is on an atomic level data can only be obtained in this spectrum. This data can be used to calculate the structure of the material. An example of the data that could be obtained during this process can be seen in **Figure Three**.

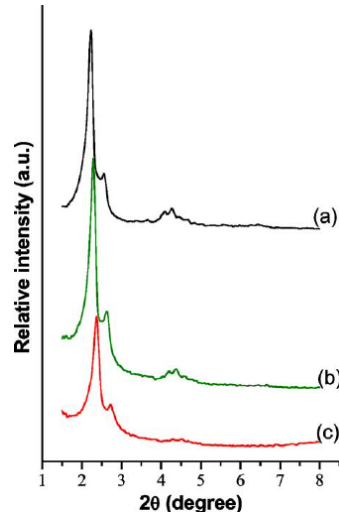


**Figure Three.** Examples of x-ray diffraction data for MCM-41

Once this process was completed, the sample was placed into a gas adsorption isotherm. The gas adsorption isotherm will measure the average pore diameter, which can be used to calculate the pore diameter. An example of data that can be obtained in this process is shown in **Figure Four**. MCM-41 is a mesoporous material that fits graph *Type IV*. Therefore the expected gas adsorption isotherm would exhibit a graph similar to graph *Type IV*.

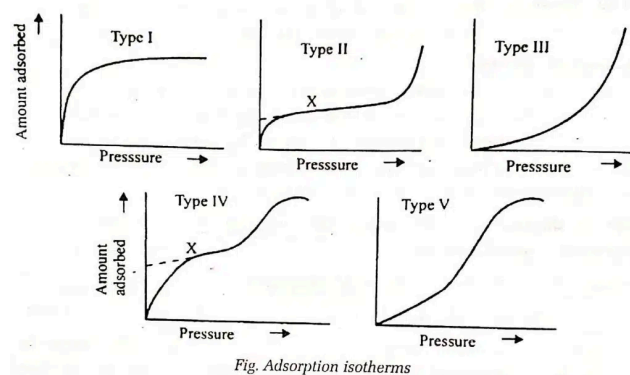


**Figure Four.** Example graphs of five types of gas adsorption isotherm data

## 2. Computational

### 2.1 Materials

To visualize the structure of the MCM-41 material coding is needed. This is due to the structure being on an interatomic level. This will be further discussed in the **Discussion & Results** section of this paper. To begin the computational work involved a computer or laptop with access to the internet is needed. Along with this, the program that was used in this research project was Python coding within JupyterLab.

### 2.2. Code

The first step in this process was to create a three-dimensional plane that would house the future 3D cube. After the 3D cube was created random seeding of circles (Representing a filled space) and triangles (Representing an unfilled space). The coding involved can be seen in **Figure(s) Five and Six**.

```
[1]: import matplotlib.pyplot as plt
import numpy as np

# Fixing random state for reproducibility
np.random.seed(19680801)

def randrange(n, vmin, vmax):
    """
    Helper function to make an array of random numbers having shape (n, )
    with each number distributed Uniform(vmin, vmax).
    """
    return (vmax - vmin)*np.random.rand(n) + vmin

fig = plt.figure()
ax = fig.add_subplot(projection='3d')

n = 100

# For each set of style and range settings, plot n random points in the box
# defined by x in [23, 32], y in [0, 100], z in [zlow, zhigh].
for m, zlow, zhigh in [('o', -50, -25), ('^', -30, -5)]:
    xs = randrange(n, 23, 32)
    ys = randrange(n, 0, 100)
    zs = randrange(n, zlow, zhigh)
    ax.scatter(xs, ys, zs, marker=m)

ax.set_xlabel('X Label')
ax.set_ylabel('Y Label')
```

**Figure Five.** Python Coding to Create 3D Plane and random seeding

```
ax.set_zlabel('Z Label')
plt.show()
```

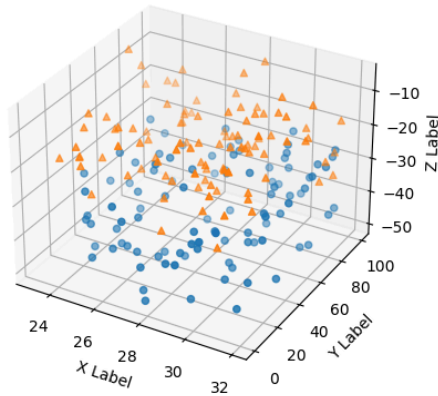


**Figure Six.** The final portion of the Python Coding and 3D Plane

Once the plane and random points were created the dimensions of the cube were created. Once the dimensions were defined, colors were associated with physical intensity. This means that the blues represents filled space and the yellows and greens represented the unfilled space. The coding involved is shown below in **Figure Seven** and the result is shown in **Figure Eight**.

```
[7]: import matplotlib.pyplot as plt
import numpy as np

# Define dimensions
Nx, Ny, Nz = 100, 100, 500
X, Y, Z = np.meshgrid(np.arange(Nx), np.arange(Ny), -np.arange(Nz))

# Create fake data
data = (((X*100)**2 + (Y*20)**2 + Z**2)/10000+1)

kw = {
    'vmin': data.min(),
    'vmax': data.max(),
    'levels': np.linspace(data.min(), data.max(), 30),
}

# Create a figure with 3D ax
fig = plt.figure(figsize=(5, 4))
ax = fig.add_subplot(111, projection='3d')

# Plot contour surfaces
ax.contourf(
    X[:, :, 0], Y[:, :, 0], data[:, :, 0],
    zdir='z', offset=0, **kw
)

ax.contourf(
    X[0, :, :], data[0, :, :], Z[0, :, :],
    zdir='y', offset=0, **kw
)

C = ax.contourf(
    data[:, :, 1], Y[:, :, 1], Z[:, :, 1],
    zdir='x', offset=X.max(), **kw
)

# --

# Set limits of the plot from coord limits
xmin, xmax = X.min(), X.max()
ymin, ymax = Y.min(), Y.max()
zmin, zmax = Z.min(), Z.max()
ax.set(xlim=[xmin, xmax], ylim=[ymin, ymax], zlim=[zmin, zmax])

# Plot edges
edges_kw = dict(color='0.4', linewidth=1, zorder=1e3)
ax.plot([xmax, xmax], [ymin, ymax], 0, **edges_kw)
ax.plot([xmin, xmax], [ymin, ymin], 0, **edges_kw)
ax.plot([xmax, xmax], [ymin, ymin], [zmin, zmax], **edges_kw)

# Set labels and ticks
ax.set(
    xlabel='X [nm]',
    ylabel='Y [nm]',
    zlabel='Z [nm]',
    zticks=[0, -250, -500, -450],
)

# Set zoom and angle view
```

**Figure Seven.** Python Coding to Code 3D Structure and Intensity Levels

```
# Set zoom and angle view
ax.view_init(40, -30, 0)
ax.set_box_aspect([None, zoom=0.9])

# Colorbar
fig.colorbar(c, ax=ax, fraction=0.02, pad=0.1, label='Name [units]')

# Show Figure
plt.show()
```

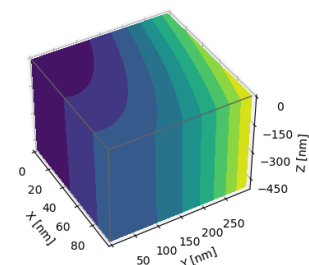


**Figure Eight.** Final Portion of Code and Structure + Intensity Colors

## Discussion & Results

The synthesized MCM-41 material was characterized through X-ray diffraction using a *D8 Advance* X-ray diffractometer at the IUMSC (Indiana University Molecular Structure Center). The *D8 Advance* is pictured below in **Figure Nine**.

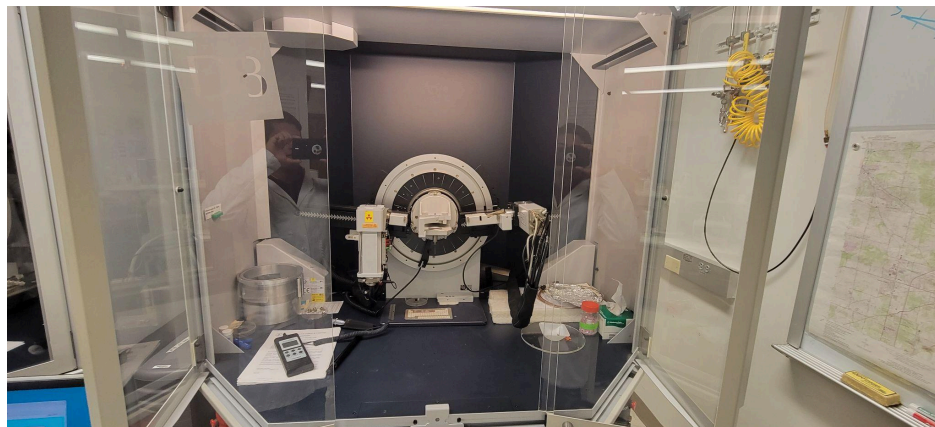


**Figure Nine.** D8 Advance X-ray Diffractometer

The way the diffractometer measures the diffraction pattern is by shooting photons at the sample and once the photons hit the MCM-41 structure the photons become scattered into X-rays which are then detected by the detector. The graph then shows the intensity of the X-rays from a 1.5-degree to 7-degree angular range. What intensity refers to is the amount of photons refracted or X-rays detected by the detector. This range was chosen to get a usable sample range due to the sub-nanoscale structure of the MCM-41 material being too small to get usable data past that angle range. MCM-41's structure is measured using Angstroms ( $\text{\AA}$ ). An Angstrom ( $10^{-10}$ ) is a tenth of a nanometer ( $10^{-9}$ ) and is mainly used to measure wavelengths and interatomic distances as discussed in section 1.3. The data obtained from the PXRD (Powder X-Ray Diffraction) from

the commercial (Sigma-Aldrich) and the synthesized MCM-41 can be seen below in **Figure(s) Ten and Eleven**.

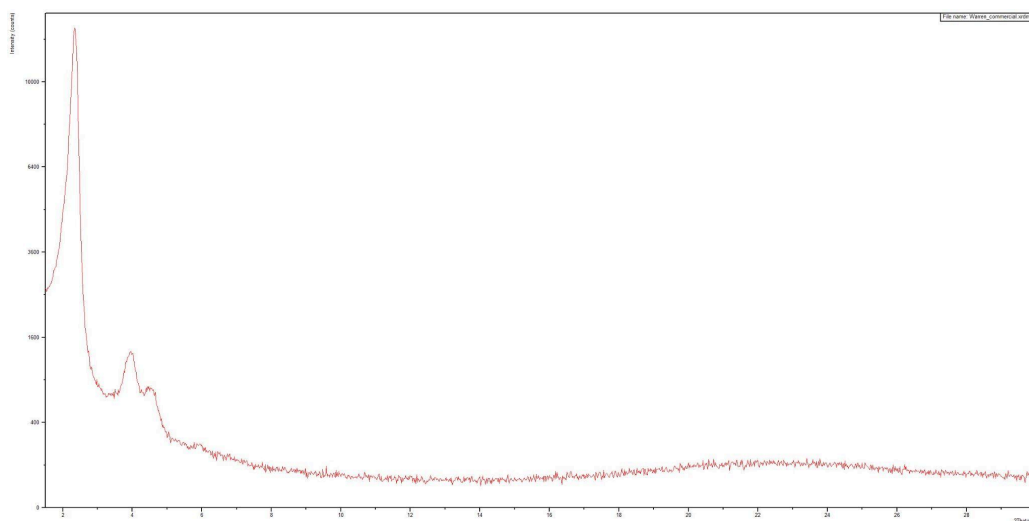


**Figure Ten.** PXRD data of the commercial MCM-41 sample

This data was measured from 1.5 to 30 degrees. The usable data can be seen between 1.5 and 12 degrees. These give great signs of MCM-41 that were made correctly. The commercial sample that was bought from Sigma-Aldrich shows the characteristics of a well-structured and ordered MCM-41 material. There is a high initial peak that shows the space between the MCM-41 pores. In all well-synthesized MCM-41 material, there is a high initial peak. This initial peak shown in the graph reaches an intensity of around 12,000 counts. The other two peaks show an MCM-41 structure, however, they are visual diffractions. As stated before, those visual diffraction peaks only verify the MCM-41 structure. PXRD was also performed on the synthesized MCM-41 material. The data obtained from the PXRD can be seen in **Figure Eleven**.

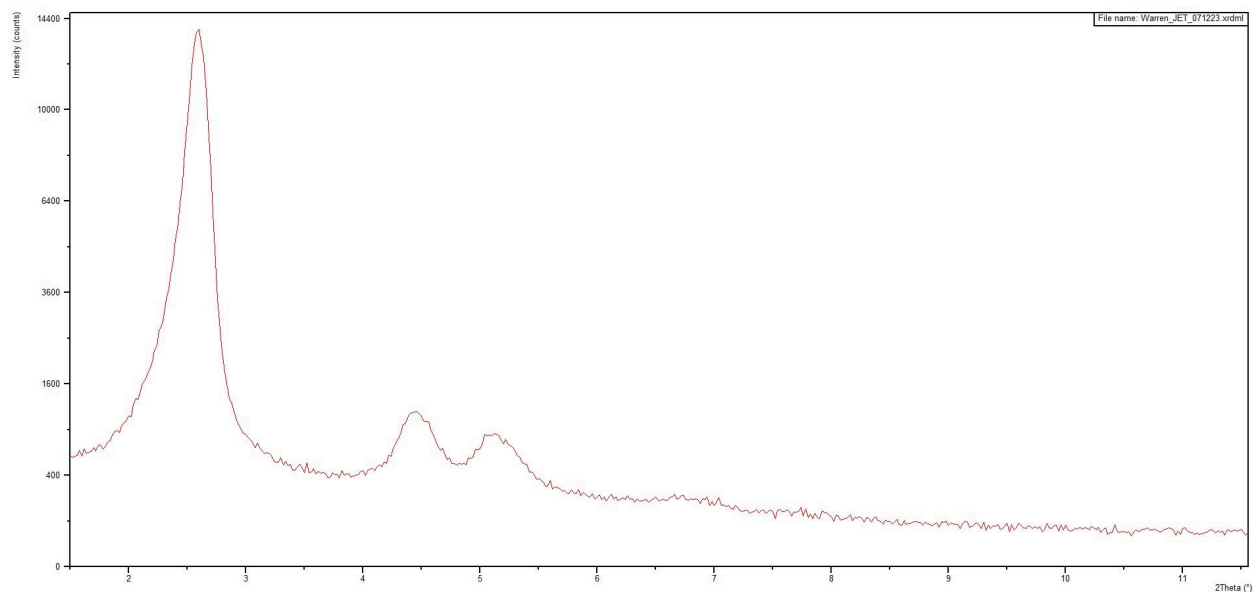


**Figure Eleven.** PXRD data from synthesized MCM-41 material

This data was obtained from a 1.5 to 12-degree angular range. The data shown in this PXRD data graph is all completely usable. As shown in the commercial (Sigma-Aldrich) MCM-41 material, there is a high initial peak. The peak is higher in the synthesized sample, around 13,000 counts compared to around 12,000 counts. What this means is that the pores of the MCM-41 structure are closer together forming a stronger structure. Also seen in this PXRD graph are the two visual diffraction peaks that verify the MCM-41 structure entirely. To truly compare this data the PXRD graphs were overlapped over each other as shown in **Figure Twelve**.

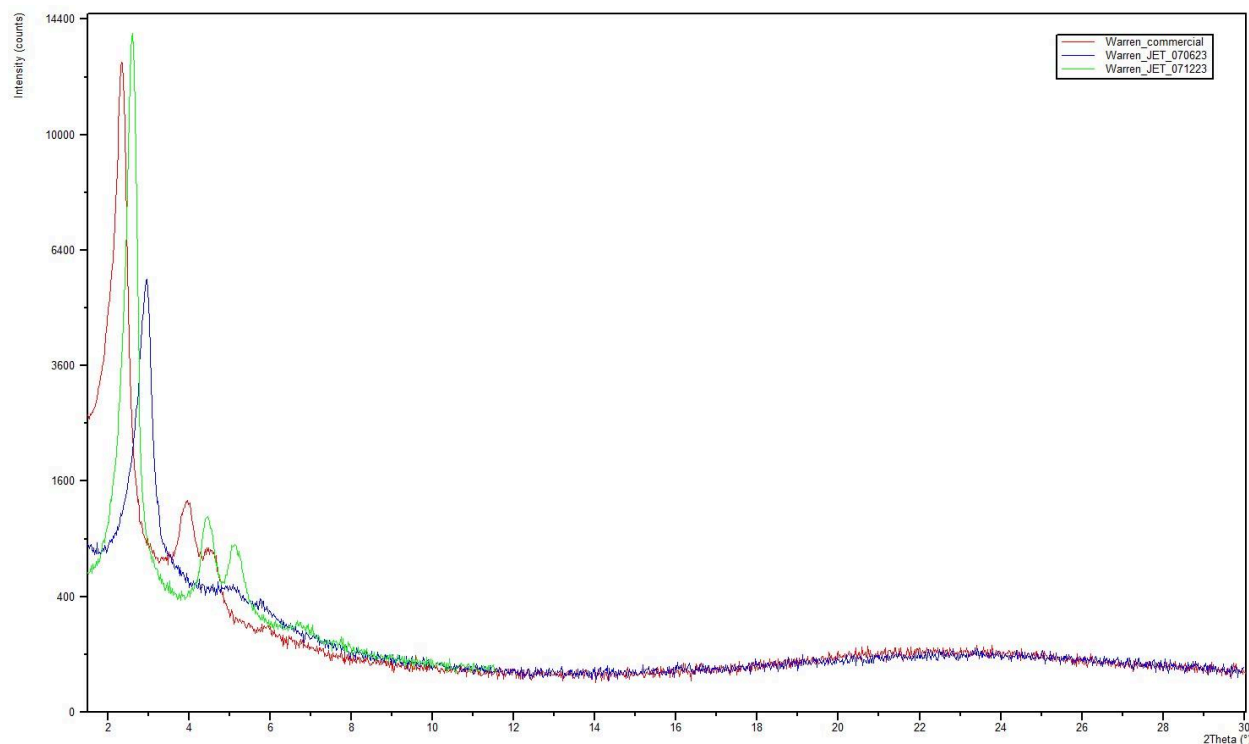


**Figure Twelve.** Overlapped PXRD data graphs

Looking at **Figure Twelve** the data shown does go above the usable range of 1.5 to twelve-degrees but results can be derived from this data. The red data represents the commercial (Sigma-Aldrich), the green data represents the synthesized MCM-41 material as discussed before, and the blue data is synthesized MCM-41 material from one of my colleagues in the Department of Physics Laboratory. Looking at the green and red data graphs are very similar and contain the three peaks that are desired. Both have a very high initial first peak that shows pore distance. The synthesized data does have a higher peak and show how well-synthesized this MCM-41 material is. And they both show two visual diffraction peaks as well. The only difference is that the synthesized material is right-shifted. This is because the distance between the atoms is less in the synthesized MCM-41 than in the commercially available sample from Sigma-Aldrich. This has a host of benefits and consequences depending on the field you want to

use this in. Furthermore, very interestingly we can compare my colleague's sample to the other two samples as well. My colleague's sample did not derive the same results as desired from them. There is an initial peak but it is smaller in counts and shows a high spacing between pores. What can also be seen is the lack of secondary and tertiary peaks. It is theorized that this is because the structure of the material collapsed at some point within the calcination process. Therefore, this sample can be used to learn more about in the sense of a failed calcination process and a collapsed structure and see what a less positive PXRD graph is.

The PXRD data shows that the synthesized material being studied in this experiment was well-made and can be used in greater research. Another step in future research is gas adsorption Isotherm. Sadly, the timeframe this experiment was held in did not allow for a gas adsorption isotherm to be performed. Although, a prediction can be made on what the gas adsorption isotherm data would look like and what the data means. As shown in **Figure Four**, the gas adsorption isotherm data would be similar to a Type IV graph that contains an “SL shape”. All mesoporous material should exhibit this graph. This shape would mean that the helium and nitrogen gas that would be put into the isotherm would attach to the surface of the walls of the pores. And initially, the temperature would need to increase and when the helium and nitrogen particles attach to the pores then the pressure would increase. This brings out the initial “S” shape. This would occur twice bringing out the “SL” shape of the data in the graph. The synthesized would most likely exhibit this type of graph. From this data, the average pore size, and pore diameter would be derived. The average pore size of most mesoporous materials is between 2-50 nanometers in size. Comparatively, MCM-41 typically has a pore size of 2-6.5 nanometers. While this is being performed since helium is being pumped into the pores the

superfluid properties would also be observed. The superfluid properties were discussed in the initial portion of the paper.

## **Conclusion**

Although the time frame of the experiment limited the amount of work that was able to be completed, many results were made that can be used in future research. With this information, there can also be different routes that this research could be taken. Different routes can be using different forms of CTAB. The CTAB used in this experiment was  $C_{16}$ TAB. Other methods do include  $C_{14}$ TAB and  $C_{12}$ TAB. Another method does include coating the pores in Cesium and/or Argon to restrict the pore size to greater emphasize the quantum state of superfluidity. Another approach to this experiment could be comparing MCM-41 to MCM-48 due to their differences in structure. In other words, the creation of MCM-41 was a success and can be used in the further production of knowledge in this ever-growing field that can benefit humanity for years to come.

**Bibliography:**

Blasco, T., Elías, V. R., Liu, C., Murrieta-Rico, F. N., Karimi, Z., Brezoiu, A.-M., Kresge, C. T., Zelenák, V., Vartuli, J. C., Puputti, J., Ciesla, U., Kim, H. J., Jones, R. H., Souza, M. J. B., Pajchel, L., Santos, L. F. S., Costa, J. A. S., Schmidt, R., Kang, K. K., ...

Pérez-Mendoza, M. (2019, September 3). *Recent progresses in the adsorption of organic, inorganic, and gas compounds by MCM-41-based mesoporous materials*. Microporous and Mesoporous Materials.

<https://nam12.safelinks.protection.outlook.com/?url=https%3A%2F%2Fwww.sciencedirect.com%2Fscience%2Farticle%2Fabs%2Fpii%2FS1387181119305554&data=05%7C01%7Cjfm Medina%40iu.edu%7Ca83f00ddd8da442cb2b708db8d5d40e8%7C1113be34aed14d00ab4bcdd02510be91%7C0%7C0%7C638259203882429093%7CUnknown%7CTWFpbGZsb3d8eyJWIjoiMC4wLjAwMDAiLCJQIjoiV2luMzIiLCJBTiI6IjEhaWwiLCJXVCi6Mn0%3D%7C3000%7C%7C%7C&sdata=6rlJo7zBTp5oLgJ8AFnSdmkO2QNG0hvrWs%2B0pRymc84%3D&reserved=0>

Del Maestro, A., Nichols, N. S., Prisk, T. R., Warren, G., & Sokol, P. E. (2017). *Experimental Realization of One Dimensional Helium*, 1–6.

Department of Physics and Astronomy, University of Tennessee, Knoxville, TN 37996, USA:  
Min H. Kao Department of Electrical Engineering and Computer Science, University of Tennessee Knoxville, TN 37996, USA Data Science and Learning Division, Argonne National Laboratory, Argonne, Illinois 60439, USA Department of Physics, University of Vermont, Burlington, VT 05405, USA Materials Science Program, University of Vermont, Burlington, VT 05404, USA Center for Neutron Research, National Institute of Standards and Technology, Gaithersburg, MD 20899-6100, USA Department of Physics, Indiana University, Bloomington, IN 47408, USA

Gabelman, A. (2017). Adsorption Basics. *Adsorption Basics: Part 1*, 48–53.

Gabelman Process Solutions, LLC

Khushalani, D., Kuperman, A., Coombs, N., & Ozin, G. A. (1996). Chem. Mater. *Mixed Surfactant Assemblies in the Synthesis of Mesoporous Silicas*, 2188–2193.

Materials Chemistry Research Group, Lash Miller Chemical Laboratories, University of Toronto, 80 St. George Street, Toronto, Ontario, Canada M5S 3H6: Central Research Catalysis Laboratory, 1776 Building, Dow Chemical Company, Midland, Michigan 48764: Imagetek: Analytical Imaging, 32 Manning Avenue, Toronto, Ontario, Canada M6J 2K4

Kumar, D., Schumacher, K., du Fresne von Hohensche, C., Grün, M., & Unger, K. K. (2001). Colloids and Surfaces A: Physicochemical and Engineering Aspects. *MCM-41, MCM-48 and Related Mesoporous Adsorbents: Their Synthesis and Characterisation*, 187–188, 109–116.

Institut für Anorganische Chemie und Analytische Chemie, Johannes Gutenberg-Universität, Duesbergweg 10-14, 55128 Mainz, Germany

Oliveira, M. R., Cecilia, J. A., De Conto, J. F., Egues, S. M., & Rodríguez-Castellón, E. (2022). FUNDAMENTALS OF SOL-GEL AND HYBRID MATERIALS PROCESSING. *Journal of Sol-Gel Science and Technology*, 105, 370–387.

Center for Studies in Colloidal Systems (NUESC), Laboratory of Materials Synthesis and Chromatography (LSINCROM), Institute of Technology and Research (ITP), Av. Murilo Dantas, 300, Aracaju, SE 49032-490, Brazil; Postgraduate Programme in Process Engineering, Tiradentes University (UNIT), Av. Murilo Dantas, 300, Aracaju, SE 49032-490, Brazil; Department of Inorganic Chemistry, Crystallography, and Mineralogy, Faculty of Sciences, University of Málaga, Avda. Cervantes, 2, 29071 Málaga, Spain

Solovyov, L. A., Belousov, O. V., Dinnebier, R. E., Shmakov, A. N., & Kirik, S. D. (2003). J. Phys. Chem B 2005. *X-Ray Diffraction Structure Analysis of MCM-48 Mesoporous Silica*, 109, 3233–3237.

Institute of Chemistry and Chemical Technology, 660049 Krasnoyarsk, Russia, Max-Planck Institute for Solid State Research, Heisenbergstrasse 1, D-70569 Stuttgart, Germany, and Borekov Institute of Catalysis, 630090 Novosibirsk, Russia

Tan, Y., & O'Haver, J. H. (2004). *Journal of Colloid and Interface Science. Use of the BET Adsorption Isotherm Equation to Examine Styrene Adsorption by Nonionic Surfactants at the Water-Silica Interface*, 279, 289–295.

Department of Chemical Engineering, the University of Mississippi, University, MS 38677, USA

Teymouri, M., Samadi-Maybodi, A., & Vahid, A. (2011). *Int. Nano Letter. A Rapid Method for the Synthesis of Highly Ordered MCM-41*, 1, 34–37.

Unknown, A. (2020). *2 Mesoporous Silica MCM-41 (Si-MCM-41)*, 95–108.

